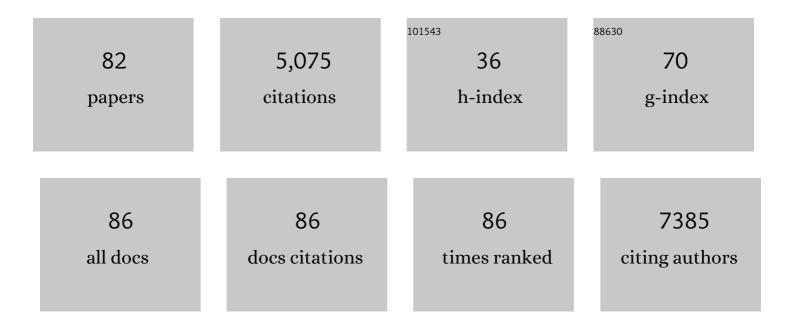
Zhanfeng Zheng

List of Publications by Year in descending order

Source: https://exaly.com/author-pdf/1996831/publications.pdf Version: 2024-02-01



#	Article	IF	CITATIONS
1	Constructing interfacial super active sites over OH-PCN/Nb2O5 heterojunction for efficient phenol photomineralization. Journal of Catalysis, 2022, 410, 63-68.	6.2	5
2	Hydrogen-Bonded Aggregates Featuring <i>n</i> → π* Electronic Transition for Efficient Visible-Light-Responsive Photocatalysis. ACS Catalysis, 2022, 12, 6276-6284.	11.2	11
3	Bidentate ligand modification strategy on supported Ni nanoparticles for photocatalytic selective hydrogenation of alkynes. Applied Catalysis B: Environmental, 2022, 313, 121449.	20.2	8
4	Strong metal-support interaction induced O2 activation over Au/MNb2O6 (M = Zn2+, Ni2+ and Co2+) for efficient photocatalytic benzyl alcohol oxidative esterification. Applied Catalysis B: Environmental, 2021, 283, 119618.	20.2	21
5	A label-free electrochemical aptasensor based on the core–shell Cu-MOF@TpBD hybrid nanoarchitecture for the sensitive detection of PDGF-BB. Analyst, The, 2021, 146, 979-988.	3.5	28
6	Hydroxyl-group-modified polymeric carbon nitride with the highly selective hydrogenation of nitrobenzene to <i>N</i> -phenylhydroxylamine under visible light. Green Chemistry, 2021, 23, 3612-3622.	9.0	22
7	Controllable Generation of Reactive Oxygen Species on Cyano-Group-Modified Carbon Nitride for Selective Epoxidation of Styrene. Innovation(China), 2021, 2, 100089.	9.1	17
8	Tailoring phenol photomineralization pathway over polymeric carbon nitride with cyano group multifunctional active sites. Applied Catalysis B: Environmental, 2021, 284, 119710.	20.2	21
9	Why phenol is selectively hydrogenated to cyclohexanol on Ru (0001): An experimental and theoretical study. Applied Surface Science, 2021, 558, 149880.	6.1	16
10	Construction of nano-TiO2 decorated titanosilicate core-shell structure: Highly efficient oxygen activation for the degradation of Rhodamine B under visible light and excellent recycling performance. Journal of Environmental Chemical Engineering, 2021, 9, 105815.	6.7	8
11	The BiOCl/diatomite composites for rapid photocatalytic degradation of ciprofloxacin: Efficiency, toxicity evaluation, mechanisms and pathways. Chemical Engineering Journal, 2020, 380, 122422.	12.7	142
12	The synergistic role of the support surface and Au–Cu alloys in a plasmonic Au–Cu@LDH photocatalyst for the oxidative esterification of benzyl alcohol with methanol. Physical Chemistry Chemical Physics, 2020, 22, 1655-1664.	2.8	14
13	Photocatalytic selective aerobic oxidation of amines to nitriles over Ru/γ-Al ₂ O ₃ : the role of the support surface and the strong imine intermediate adsorption. Catalysis Science and Technology, 2020, 10, 440-449.	4.1	22
14	Plasmon-enhanced furfural hydrogenation catalyzed by stable carbon-coated copper nanoparticles driven from metal–organic frameworks. Catalysis Science and Technology, 2020, 10, 6483-6494.	4.1	23
15	Light assisted O-alkylation of phenols to ethers using layered double oxides catalyst under green and mild conditions. Journal of Photochemistry and Photobiology A: Chemistry, 2020, 400, 112695.	3.9	2
16	Efficient photocatalytic oxidative deamination of imine and amine to aldehyde over nitrogen-doped KTi3NbO9 under purple light. Catalysis Science and Technology, 2020, 10, 6611-6617.	4.1	5
17	Visible-light-driven Hydroamination of Alkynes over a New Type of Activated Carbon Immobilized Cu2+ Photocatalyst. Chemical Research in Chinese Universities, 2020, 36, 1039-1044.	2.6	2
18	Defect Engineering in Pd/NiCo ₂ O _{4–<i>x</i>} for Selective Hydrogenation of α,β-Unsaturated Carbonyl Compounds under Ambient Conditions. ACS Sustainable Chemistry and Engineering, 2020, 8, 7851-7859.	6.7	29

#	Article	IF	CITATIONS
19	The key role of photoisomerisation for the highly selective photocatalytic hydrogenation of azobenzene to hydrazobenzene over NaNbO3 fibre photocatalyst. Journal of Photochemistry and Photobiology A: Chemistry, 2020, 400, 112655.	3.9	6
20	Differences in the selective reduction mechanism of 4-nitroacetophenone catalysed by rutile- and anatase-supported ruthenium catalysts. Catalysis Science and Technology, 2020, 10, 1518-1528.	4.1	12
21	Oxygen vacancies confined in conjugated polyimide for promoted visible-light photocatalytic oxidative coupling of amines. Applied Catalysis B: Environmental, 2020, 272, 118964.	20.2	54
22	A Sensitive Electrochemical MUC1 Sensing Platform Based on Electroactive Cu-MOFs Decorated by AuPt Nanoparticles. Journal of the Electrochemical Society, 2020, 167, 087502.	2.9	8
23	A Density Functional Theory Study on the Acidâ€Catalyzed Transesterification Mechanism for Biodiesel Production from Waste Cooking Oils. JAOCS, Journal of the American Oil Chemists' Society, 2019, 96, 137-145.	1.9	5
24	Conjugated HCl-doped polyaniline for photocatalytic oxidative coupling of amines under visible light. Catalysis Science and Technology, 2019, 9, 753-761.	4.1	40
25	BiOBr-photocatalyzedcis–transisomerization of 9-octadecenoic acids in different atmospheres. Catalysis Science and Technology, 2019, 9, 3380-3387.	4.1	4
26	Enhanced photocatalytic reduction of CO ₂ to CO over BiOBr assisted by phenolic resin-based activated carbon spheres. RSC Advances, 2019, 9, 14391-14399.	3.6	28
27	Light-assisted <i>O</i> -methylation of phenol with dimethyl carbonate over a layered double oxide catalyst. Catalysis Science and Technology, 2019, 9, 1774-1778.	4.1	12
28	One-pot selective synthesis of azoxy compounds and imines via the photoredox reaction of nitroaromatic compounds and amines in water. Scientific Reports, 2019, 9, 1280.	3.3	10
29	ZnNb ₂ O ₆ fibre surface as an efficiently product-selective controller for the near-UV-light-induced nitrobenzene reduction reaction. Catalysis Science and Technology, 2019, 9, 6681-6690.	4.1	15
30	Enhanced photocatalytic hydrogen production from aqueous-phase methanol reforming over cyano-carboxylic bifunctionally-modified carbon nitride. Chemical Communications, 2019, 55, 12503-12506.	4.1	22
31	Theoretical insights into photo-induced electron transfer at BiOX (X = F, Cl, Br, I) (001) surfaces and interfaces. Physical Chemistry Chemical Physics, 2019, 21, 868-875.	2.8	51
32	Cyano group modified carbon nitride with enhanced photoactivity for selective oxidation of benzylamine. Applied Catalysis B: Environmental, 2019, 242, 67-75.	20.2	87
33	A novel K2Ti8O17 nanorod photocatalyst rich in surface OH groups for efficient hydrogen production by water splitting. International Journal of Hydrogen Energy, 2018, 43, 18115-18124.	7.1	11
34	Dual modification of TiNb ₂ O ₇ with nitrogen dopants and oxygen vacancies for selective aerobic oxidation of benzylamine to imine under green light. Journal of Materials Chemistry A, 2017, 5, 4607-4615.	10.3	60
35	Graphene-supported CoS ₂ particles: an efficient photocatalyst for selective hydrogenation of nitroaromatics in visible light. Catalysis Science and Technology, 2017, 7, 2805-2812.	4.1	40
36	Graphene oxide/core–shell structured metal–organic framework nano-sandwiches and their derived cobalt/N-doped carbon nanosheets for oxygen reduction reactions. Journal of Materials Chemistry A, 2017, 5, 10182-10189.	10.3	163

#	Article	IF	CITATIONS
37	Porous TiO 2 Nanotubes with Spatially Separated Platinum and CoO x Cocatalysts Produced by Atomic Layer Deposition for Photocatalytic Hydrogen Production. Angewandte Chemie, 2017, 129, 834-838.	2.0	16
38	Porous TiO ₂ Nanotubes with Spatially Separated Platinum and CoO _x Cocatalysts Produced by Atomic Layer Deposition for Photocatalytic Hydrogen Production. Angewandte Chemie - International Edition, 2017, 56, 816-820.	13.8	293
39	Simulation-guided synthesis of graphitic carbon nitride beads with 3D interconnected and continuous meso/macropore channels for enhanced light absorption and photocatalytic performance. Journal of Materials Chemistry A, 2017, 5, 21300-21312.	10.3	63
40	New Approach to Create TiO ₂ (B)/Carbon Core/Shell Nanotubes: Ideal Structure for Enhanced Lithium Ion Storage. ACS Applied Materials & Interfaces, 2016, 8, 18815-18821.	8.0	37
41	The crystallography of C-centred monoclinic to body-centred tetragonal polymorphic phase transformation in mixed-phase TiO 2 (B) and anatase nanocomposite. Scripta Materialia, 2016, 119, 27-32.	5.2	11
42	Efficient Removal of Cationic and Anionic Radioactive Pollutants from Water Using Hydrotalcite-Based Getters. ACS Applied Materials & Interfaces, 2016, 8, 16503-16510.	8.0	40
43	Alloying Gold with Copper Makes for a Highly Selective Visible-Light Photocatalyst for the Reduction of Nitroaromatics to Anilines. ACS Catalysis, 2016, 6, 1744-1753.	11.2	164
44	Factors influencing the photocatalytic hydroamination of alkynes with anilines catalyzed by supported gold nanoparticles under visible light irradiation. RSC Advances, 2016, 6, 31717-31725.	3.6	9
45	Probing the mechanism of benzaldehyde reduction to chiral hydrobenzoin on the CNT surface under near-UV light irradiation. Green Chemistry, 2016, 18, 1482-1487.	9.0	26
46	Heterojunctions between amorphous and crystalline niobium oxide with enhanced photoactivity for selective aerobic oxidation of benzylamine to imine under visible light. Journal of Materials Chemistry A, 2015, 3, 18045-18052.	10.3	68
47	Surface-mediated selective photocatalytic aerobic oxidation reactions on TiO ₂ nanofibres. RSC Advances, 2015, 5, 56820-56831.	3.6	11
48	Revisiting the CO Oxidation Reaction on Various Au/TiO ₂ Catalysts: Roles of the Surface OH Groups and the Reaction Mechanism. Journal of Nanoscience and Nanotechnology, 2014, 14, 6885-6893.	0.9	6
49	Heterojunctions in g-C ₃ N ₄ /TiO ₂ (B) nanofibres with exposed (001) plane and enhanced visible-light photoactivity. Journal of Materials Chemistry A, 2014, 2, 2071-2078.	10.3	241
50	TiO2 nanofibers of different crystal phases for transesterification of alcohols with dimethyl carbonate. Applied Catalysis B: Environmental, 2014, 150-151, 330-337.	20.2	32
51	Viable Photocatalysts under Solarâ€Spectrum Irradiation: Nonplasmonic Metal Nanoparticles. Angewandte Chemie - International Edition, 2014, 53, 2935-2940.	13.8	234
52	Visibleâ€Lightâ€Induced Selective Photocatalytic Oxidation of Benzylamine into Imine over Supported Ag/AgI Photocatalysts. ChemCatChem, 2014, 6, 1210-1214.	3.7	24
53	Tunneling STM/STS and break-junction spectroscopy of the layered nitro-chloride superconductors <i>M</i> NCl (<i>M</i> = Ti, Hf, Zr). Journal of Physics: Conference Series, 2014, 507, 012010.	0.4	0
54	Silver oxide nanocrystals anchored on titanate nanotubes and nanofibers: promising candidates for entrapment of radioactive iodine anions. Nanoscale, 2013, 5, 11011.	5.6	64

#	Article	IF	CITATIONS
55	Removal of radioactive iodine from water using Ag2O grafted titanate nanolamina as efficient adsorbent. Journal of Hazardous Materials, 2013, 246-247, 199-205.	12.4	92
56	Painting Anatase (TiO ₂) Nanocrystals on Long Nanofibers to Prepare Photocatalysts with Large Active Surface for Dye Degradation and Organic Synthesis. ChemCatChem, 2013, 5, 2382-2388.	3.7	9
57	Highly efficient and selective photocatalytic hydroamination of alkynes by supported gold nanoparticles using visible light at ambient temperature. Chemical Communications, 2013, 49, 2676.	4.1	76
58	Titanate-based adsorbents for radioactive ions entrapment from water. Nanoscale, 2013, 5, 2232.	5.6	102
59	Enhancing Photoactivity of TiO ₂ (B)/Anatase Core–Shell Nanofibers by Selectively Doping Cerium Ions into the TiO ₂ (B) Core. Chemistry - A European Journal, 2013, 19, 5113-5119.	3.3	51
60	Free-standing and bendable carbon nanotubes/TiO2 nanofibres composite electrodes for flexible lithium ion batteries. Electrochimica Acta, 2013, 104, 41-47.	5.2	64
61	Superconducting β-ZrNClx probed by scanning-tunnelling and break-junction spectroscopy. Physica C: Superconductivity and Its Applications, 2013, 494, 89-94.	1.2	6
62	Tuning the Surface Structure of Nitrogenâ€Doped TiO ₂ Nanofibres—An Effective Method to Enhance Photocatalytic Activities of Visibleâ€Lightâ€Driven Green Synthesis and Degradation. Chemistry - A European Journal, 2013, 19, 5731-5741.	3.3	31
63	STM/STS Observation on Layered Nitride Superconductor α-(DDA) _{<i>x</i>} TiNCl. Journal of Physics: Conference Series, 2012, 400, 022112.	0.4	1
64	Preparation and superconductivity of intercalation compounds of TiNCl with aliphatic amines. Journal of Materials Chemistry, 2012, 22, 10752.	6.7	18
65	xmins:mmi= http://www.w3.org/1998/Math/Math/Math/Math/Math/Math/Math/Math	3.2	28
66	Driving selective aerobic oxidation of alkyl aromatics by sunlight on alcohol grafted metal hydroxides. Chemical Science, 2012, 3, 2138.	7.4	61
67	Preparation and Superconductivity of New Stage and Polytypic Phases in Potassium-Intercalated Zirconium Nitride Chloride (K _{<i>x</i>) Sub>ZrNCl). Chemistry of Materials, 2011, 23, 1558-1563.}	6.7	11
68	Grafting silica species on anatase surface for visible light photocatalytic activity. Energy and Environmental Science, 2011, 4, 2279.	30.8	46
69	Capture of Radioactive Cesium and Iodide Ions from Water by Using Titanate Nanofibers and Nanotubes. Angewandte Chemie - International Edition, 2011, 50, 10594-10598.	13.8	208
70	Correlation of the Catalytic Activity for Oxidation Taking Place on Various TiO ₂ Surfaces with Surface OH Groups and Surface Oxygen Vacancies. Chemistry - A European Journal, 2010, 16, 1202-1211.	3.3	103
71	A Raman spectroscopic and TEM study on the structural evolution of Na ₂ Ti ₃ O ₇ during the transition to Na ₂ Ti ₆ O ₁₃ . Journal of Raman Spectroscopy, 2010, 41, 1331-1337.	2.5	84
72	A Raman spectroscopic study on the allocation of ammonium adsorbing sites on H ₂ Ti ₃ O ₇ nanofibre and its structural derivation during calcination. Journal of Raman Spectroscopy, 2010, 41, 1601-1605.	2.5	17

#	Article	IF	CITATIONS
73	A Raman spectroscopic study on the active site of sodium cations in the structure of Na ₂ Ti ₃ O ₇ during the adsorption of Sr ²⁺ and Ba ²⁺ cations. Journal of Raman Spectroscopy, 2010, 41, 1792-1796.	2.5	31
74	Structure and contribution to photocatalytic activity of the interfaces in nanofibers with mixed anatase and TiO2(B) phases. Journal of Molecular Catalysis A, 2010, 316, 75-82.	4.8	79
75	Sorption induced structural deformation of sodium hexa-titanate nanofibers and their ability to selectively trap radioactive Ra(ii) ions from water. Physical Chemistry Chemical Physics, 2010, 12, 1271-1277.	2.8	58
76	Coherent Interfaces between Crystals in Nanocrystal Composites. ACS Nano, 2010, 4, 6219-6227.	14.6	46
77	Supported silver nanoparticles as photocatalysts under ultraviolet and visible light irradiation. Green Chemistry, 2010, 12, 414.	9.0	296
78	TEM Investigation and FBB Model Explanation to the Phase Relationships between Titanates and Titanium Dioxides. Journal of Physical Chemistry C, 2010, 114, 11430-11434.	3.1	16
79	An Efficient Photocatalyst Structure: TiO ₂ (B) Nanofibers with a Shell of Anatase Nanocrystals. Journal of the American Chemical Society, 2009, 131, 17885-17893.	13.7	482
80	Mechanism of supported gold nanoparticles as photocatalysts under ultraviolet and visible light irradiation. Chemical Communications, 2009, , 7524.	4.1	267
81	Layered Titanate Nanofibers as Efficient Adsorbents for Removal of Toxic Radioactive and Heavy Metal Ions from Water. Journal of Physical Chemistry C, 2008, 112, 16275-16280.	3.1	185
82	Structural Evolution in a Hydrothermal Reaction between Nb2O5and NaOH Solution:Â From Nb2O5Grains to Microporous Na2Nb2O6·2/3H2O Fibers and NaNbO3Cubes. Journal of the American Chemical Society, 2006, 128, 2373-2384.	13.7	182